

Brain injury in combination with tacrolimus promotes the regeneration of injured peripheral nerves

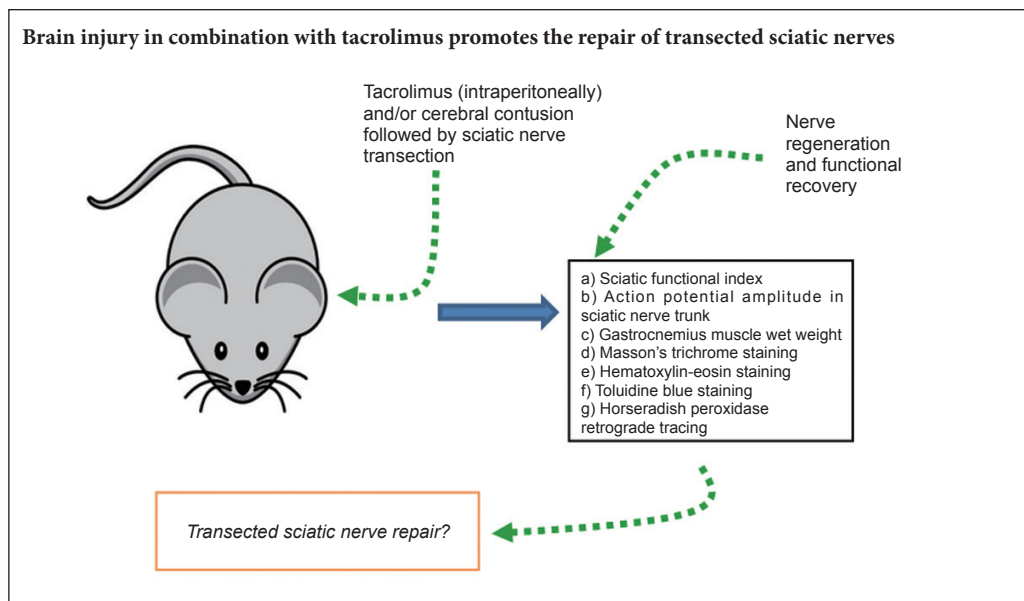
Xin-ze He^{1,5}, Jian-jun Ma², Hao-qi Wang², Tie-min Hu³, Bo Sun¹, Yun-feng Gao¹, Shi-bo Liu¹, Wei Wang⁴, Pei Wang^{1,*}

1 Department of Hand and Foot Surgery, Affiliated Hospital of Chengde Medical College, Chengde, Hebei Province, China
2 Postgraduate School, Chengde Medical College, Chengde, Hebei Province, China
3 Department of Neurosurgery, Affiliated Hospital of Chengde Medical College, Chengde, Hebei Province, China
4 Department of Hand and Foot Surgery, the First Hospital of Qinhuangdao, Qinhuangdao, Hebei Province, China
5 Binzhou Central Hospital, Binzhou, Shandong Province, China

How to cite this article: He XZ, Ma JJ, Wang HQ, Hu TM, Sun B, Gao YF, Liu SB, Wang W, Wang P (2017) Brain injury in combination with tacrolimus promotes the regeneration of injured peripheral nerves. *Neural Regen Res* 12(6):987-994.

Funding: This work was supported by a grant from the Mandatory Project of Health Department of Hebei Province of China, No. 20130027; a grant from the Mandatory Project of Science and Technology Department of Hebei Province of China, No. 142777105D; a grant from Science and Technology Bureau of Chengde City of Hebei Province of China, No. 20123128.

Graphical Abstract



*Correspondence to:
Pei Wang, cdgkwp@sina.com.

orcid:
0000-0002-0597-546X
(Pei Wang)

doi: 10.4103/1673-5374.208595

Accepted: 2017-04-14

Abstract

Both brain injury and tacrolimus have been reported to promote the regeneration of injured peripheral nerves. In this study, before transection of rat sciatic nerve, moderate brain contusion was (or was not) induced. After sciatic nerve injury, tacrolimus, an immunosuppressant, was (or was not) intraperitoneally administered. At 4, 8 and 12 weeks after surgery, Masson's trichrome, hematoxylin-eosin, and toluidine blue staining results revealed that brain injury or tacrolimus alone or their combination alleviated gastrocnemius muscle atrophy and sciatic nerve fiber impairment on the experimental side, simultaneously improved sciatic nerve function, and increased gastrocnemius muscle wet weight on the experimental side. At 8 and 12 weeks after surgery, brain injury induction and/or tacrolimus treatment increased action potential amplitude in the sciatic nerve trunk. Horseradish peroxidase retrograde tracing revealed that the number of horseradish peroxidase-positive neurons in the anterior horn of the spinal cord was greatly increased. Brain injury in combination with tacrolimus exhibited better effects on repair of injured peripheral nerves than brain injury or tacrolimus alone. This result suggests that brain injury in combination with tacrolimus promotes repair of peripheral nerve injury.

Key Words: nerve regeneration; brain injury; peripheral nerve; tacrolimus; toluidine blue staining; retrograde tracing; muscle atrophy; neural regeneration

Introduction

Brain injury is commonly associated with peripheral nerve damage (He et al., 2016). Brain injury has been shown to promote recovery of damaged peripheral nerves (Wang et al., 2014), however, the specific mechanism is not clear.

The immunosuppressant tacrolimus has been used to reduce immune rejection after organ transplantation. Tacrolimus was first reported by Gold et al. (1994) to promote the regeneration of damaged peripheral nerves. Since then, several studies (Glaus et al., 2011; Mekaj et al., 2014, 2015a, b; Phillips

et al., 2014; Zhao et al., 2014) have confirmed that tacrolimus contributes to peripheral nerve regeneration *via* immunosuppressive and neurotrophic pathways. It forms a complex with the binding region of tacrolimus binding protein (FKBP12), and then combines with the functional region of that protein, which increases the expression of growth associated protein-43 and contributes to the formation and extension of growth cones. Previous studies have shown that as damaged peripheral nerves recovered after treatment with tacrolimus, action potentials began to reach target organs again, the inner diameter of the regenerated axon increased, the myelin sheath thickened, and the amplitude of action potentials increased (Mekaj et al., 2014; Carrasco et al., 2016).

In the present study, we investigated whether brain injury in combination with tacrolimus exhibits better effects on promoting regeneration of injured peripheral nerves than brain injury or tacrolimus alone.

Materials and Methods

Ethics statement

The study protocol was approved by the Ethics Committee of the Affiliated Hospital of Chengde Medical College, China (Approval No. C20160201). The experimental procedure

followed the National Institutes of Health Guide for the Care and Use of Laboratory Animals (NIH Publications No. 8023, revised 1978).

Animals

The experiments were performed in the Affiliated Hospital of Chengde Medical College, China, from October 2015 to February 2016. We used 180 male, specific-pathogen-free Sprague-Dawley rats, aged 8 weeks and weighing 200–220 g (Vital River, Beijing, China; license No. SCXK (Jing) 2012-0001). The rats were housed at $23 \pm 2^\circ\text{C}$ under a 12-hour light/dark cycle. Rats were randomly assigned to four equal groups with 45 rats in each group: A1 (brain injury + sciatic nerve injury + tacrolimus), A2 (brain injury + sciatic nerve injury), B1 (sciatic nerve injury + tacrolimus), B2 (sciatic nerve injury alone).

Establishment of rat models of brain injury combined with sciatic nerve injury

Rats were injected with cefazolin sodium (100 mg/kg intramuscularly) 30 minutes before surgery. Surgical area was shaved. Rats were anesthetized with 10% chloral hydrate (3.5 mL/kg intraperitoneally) immediately before surgery. The sur-



Figure 1 Hindpaw ulceration 12 weeks after surgery. (A) Brain injury + sciatic nerve injury + tacrolimus; (B) brain injury + sciatic nerve injury; (C) sciatic nerve injury + tacrolimus; (D) sciatic nerve injury alone. Arrows show skin ulcers.

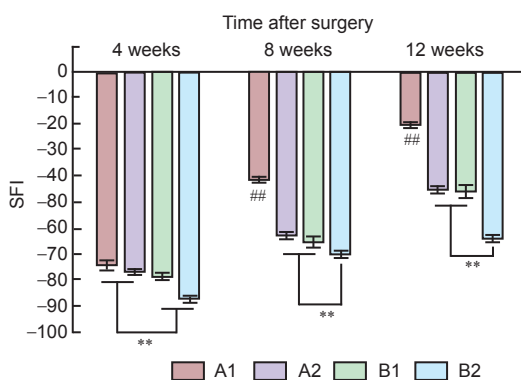


Figure 2 Sciatic function of rats with sciatic nerve injury following brain injury induction and/or tacrolimus treatment.

At 4 weeks after surgery, SFI was better in groups A1 and A2 than in groups B1 and B2 (** $P < 0.01$). At 8 and 12 weeks, SFI was better in groups A2 and B1 than in group B2 (** $P < 0.01$) and better in group A1 than in all other groups (### $P < 0.01$, vs. other three groups). Data expressed as the mean \pm SD were analyzed by one-way analysis of variance followed by the Student-Newman-Keuls test. SFI: 0, normal function; -100, complete dysfunction. Group A1: Brain injury + sciatic nerve injury + tacrolimus; group A2: brain injury + sciatic nerve injury; group B1: sciatic nerve injury + tacrolimus; group B2: sciatic nerve injury alone. SFI: Sciatic functional index.

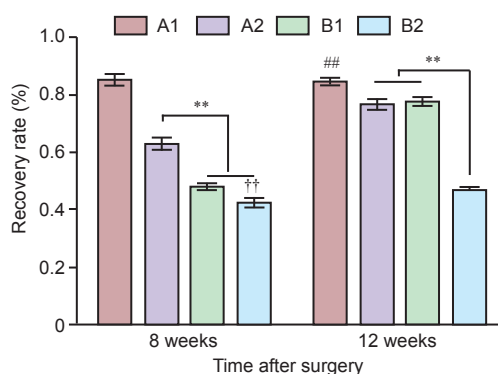


Figure 3 Recovery rate (%) of action potential amplitude in the sciatic nerve trunk in rats with sciatic nerve injury following brain injury induction and/or tacrolimus treatment.

At 8 weeks after surgery, recovery was better in group A2 than in groups B1 and B2 (** $P < 0.01$), and better in group B1 than in B2 ($\dagger\dagger P < 0.01$, vs. group B1). At 12 weeks after surgery, recovery was better in group A1 than in all other groups (### $P < 0.01$, vs. other three groups). Groups A2 and B1 also showed better recovery than group B2 (** $P < 0.01$). Data expressed as the mean \pm SD were analyzed by one-way analysis of variance followed by the Student-Newman-Keuls test. Recovery rate of action potential amplitude = action potential amplitude recorded by stimulating electrode 1/action potential amplitude recorded by stimulating electrode 2 \times 100%. Group A1: Brain injury + sciatic nerve injury + tacrolimus; group A2: brain injury + sciatic nerve injury; group B1: sciatic nerve injury + tacrolimus; group B2: sciatic nerve injury alone.

gical area was disinfected, and an aseptic towel was placed over the head with an aperture over the surgical site. A sagittal skin incision was made on the head, and a bone window (5 mm in diameter, 1.5 mm posterior to the coronal suture, and 5 mm to the left of the midline) was opened. A moderate contusion injury was induced using Feeney's method (Feeney et al., 1981). The right sciatic nerve of rats was exposed, transected 1 cm below the lower hole of the piriformis of the rats, and then sutured with 9-0 nontraumatic thread using an epicardial suture technique under a surgical microscope (LZL-6A; Zhenjiang Zhongtian Optical instrument Co., Ltd., Zhenjiang, Jiangsu Province, China) at 12× magnification. The epineurium of the sciatic nerve was closed with 4–6 stitches using a 9/0 sterile medical non-absorbable sutures and non-destructive suture needle (Hangzhou Fu Yang Medical Suture Needle Factory, Hangzhou, Zhejiang Province, China) (Cheng et al., 2015).

Tacrolimus administration

Twelve hours after surgery, rats in groups A1 and B1 (n = 45 per group) were injected with tacrolimus (Selleck Chemicals, Houston, TX, USA; 5 mg/kg intraperitoneally) daily for 2 weeks. Rats in groups A2 and B2 (n = 45 per group) were injected intraperitoneally with an equivalent volume (5 mL/kg) of physiological saline under the same schedule.

Measurement of sciatic functional index (SFI)

At 4, 8 and 12 weeks after sciatic nerve transection, 10 rats were randomly selected from each group. According to a previous method (Phillips et al., 2014), we measured the podogram length, toe separation, and inter-toe distance on

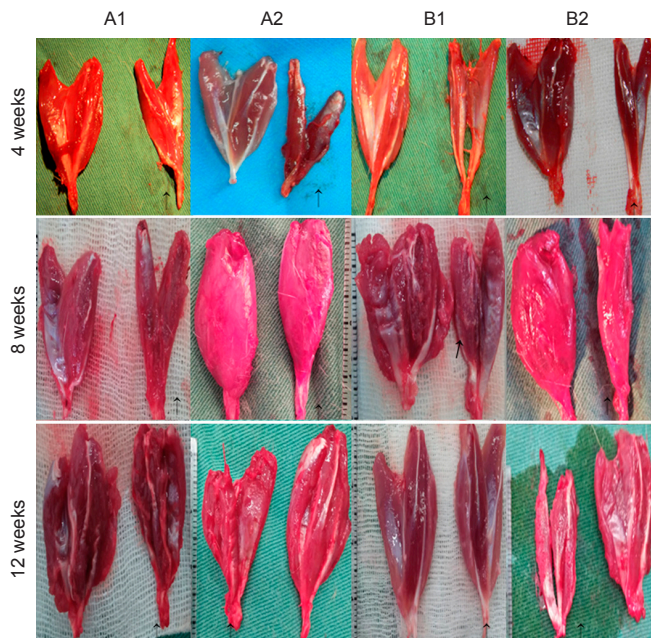


Figure 4 Denervated (arrows) and contralateral (unlabeled) gastrocnemius muscles of rats with sciatic nerve injury following brain injury induction and/or tacrolimus treatment.

At 4 weeks after surgery, muscle wet weight recovery rate was greater in group A1 than in all other groups. At 8 and 12 weeks after surgery, muscle wet weight recovery rate was markedly better in groups A1, A2 and B1 than in group B2. Group A1: Brain injury + sciatic nerve injury + tacrolimus; group A2: brain injury + sciatic nerve injury; group B1: sciatic nerve injury + tacrolimus; group B2: sciatic nerve injury alone.

the experimental and contralateral sides. Sciatic functional index (SFI) = $[-38.3 \times (PL_E - PL_C) / PL_C] + [109.5 \times (TS_E - TS_C) / TS_C] + [13.2 \times (IT_E - IT_C) / IT_C] - 8.8$, in which PL, podogram length; TS, toe separation; IT, inter-toe distance; E, experimental side; C, contralateral side. SFI: 0, normal function; -100, complete dysfunction.

Recovery rate of action potential amplitude in sciatic nerve trunk

At 8 and 12 weeks after sciatic nerve surgery, five rats were randomly selected from each group. Stimulating electrode 1 was placed 0.5 cm distal to the anastomotic stoma, and stimulating electrode 2 was placed 3 mm proximal to it. The recording electrodes were placed near the nerve root. Electrical signal was input directly into the BL-420F bio-function experiment system (Chengdu Techman Software Co., Ltd., Chengdu, Sichuan Province, China). The recovery rate of action potential amplitude in the sciatic nerve trunk was calculated to assess nerve regeneration (Schiaveto de Souza et al., 2004). Recovery rate of action potential amplitude = action potential amplitude recorded by stimulating electrode 1 / action potential amplitude recorded by stimulating electrode 2 × 100%.

Recovery rate of gastrocnemius muscle wet weight

At 4, 8 and 12 weeks after sciatic nerve surgery, five rats were randomly selected from each group and sacrificed with an overdose of anesthetic. Bilateral gastrocnemius muscle was harvested and blotted with absorbent paper. The size and color of the muscle were observed, and the wet weight was weighed and used to determine muscle atrophy and recovery rate (the wet weight of gastrocnemius muscle on the experimental side / the wet weight of gastrocnemius muscle on the

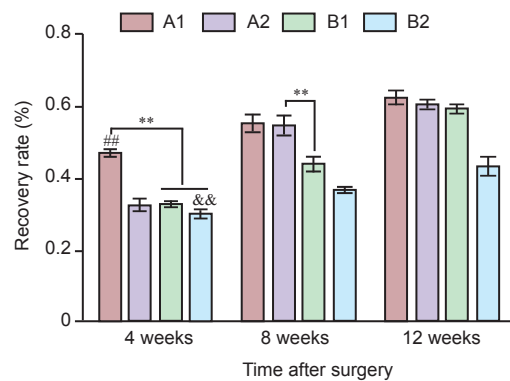


Figure 5 Recovery rate (%) of gastrocnemius muscle wet weight in rats with sciatic nerve injury following brain injury induction and/or tacrolimus treatment.

At 4 weeks after surgery, the recovery of gastrocnemius muscle was better in group A1 than in all other groups (###P < 0.01, vs. other three groups). Recovery was better in group A1 than in groups B1 and B2 (**P < 0.01), and better in groups A2 and B1 than in group B2 (&&P < 0.01, vs. groups A2 and B1). At 8 weeks after surgery, gastrocnemius muscle recovery was better in group A2 than in group B1 (**P < 0.01). Data expressed as the mean ± SD were analyzed by one-way analysis of variance followed by the Student-Newman-Keuls test. Recovery rate (%) of gastrocnemius muscle wet weight = the wet weight of gastrocnemius muscle on the experimental side / the wet weight of gastrocnemius muscle on the contralateral side × 100%. Group A1: Brain injury + sciatic nerve injury + tacrolimus; group A2: brain injury + sciatic nerve injury; group B1: sciatic nerve injury + tacrolimus; group B2: sciatic nerve injury alone.

contralateral side \times 100%) during nerve regeneration.

Masson's trichrome staining of gastrocnemius muscle

At 4, 8 and 12 weeks after sciatic nerve surgery, five rats were randomly selected from each group. After sacrificing the animals using an overdose of anesthesia, denervated skeletal muscle was collected, fixed in 10% formaldehyde for 24 hours, dehydrated, embedded in paraffin, and cut into 5 μ m-thick transverse sections. These sections were stained using a Masson's trichrome kit (Jiangsu KeyGen Biotech Co., Ltd., Nanjing, Jiangsu Province, China) according to the manufacturer's instructions, mounted, and observed under the light microscope (BH-3; Olympus, Tokyo, Japan) to assess the recovery of the denervated muscle.

Hematoxylin-eosin staining of sciatic nerve

At 4, 8 and 12 weeks after surgery, five rats were randomly selected from each group. Tissue 0.5 cm distal to the anastomotic stoma was fixed in 10% formaldehyde for 24 hours, dehydrated through a graded alcohol series, embedded in paraffin, and sliced into 5 μ m-thick transverse sections. These sections were stained with hematoxylin and eosin, permeabilized in xylene, and mounted. Schwann cells and nerve fibers were observed under the light microscope (BH-3; Olympus) to evaluate regeneration.

Masson's trichrome staining of sciatic nerve

At 4, 8 and 12 weeks after surgery, five rats were randomly selected from each group and sacrificed using an overdose of anesthesia. Tissue 0.5 cm distal to the anastomotic stoma was fixed in 10% formaldehyde for 24 hours, dehydrated through a graded alcohol series, embedded in paraffin, and cut into 5 μ m-thick transverse sections. The sections were stained with a Masson's trichrome kit (standard type; Jiangsu KeyGen Biotech Co., Ltd., Nanjing, Jiangsu Province, China) according to the manufacturer's instructions. Nerve and collagen fiber proliferation was observed under the light microscope (BH-3; Olympus).

Toluidine blue staining of sciatic nerve

At 4, 8 and 12 weeks after surgery, five rats were randomly selected from each group. Sciatic nerve tissue 0.5 cm distal to the anastomotic stoma was fixed in 10% formaldehyde for 24 hours, dehydrated through a graded alcohol series, embedded in paraffin, and cut into 4 μ m-thick transverse sections. The sections were stained with 1% toluidine blue (Sigma, St. Louis, MO, USA) for 20 minutes, treated with alcohol for rapid color separation, permeabilized with xylene, and mounted. Remyelination of nerve fibers was observed under the light microscope (BH-3; Olympus).

Horseradish peroxidase (HRP) tracing

At 8 and 12 weeks after surgery, 5 μ L 30% HRP was infused into the tissue 0.5 cm distal to the sciatic nerve stump. Thoracotomy was conducted under deep anesthesia. Warm physiological saline (150 mL) was perfused rapidly through the left ventricle to wash the blood vessels, and tissues were fixed with 500 mL 2% paraformaldehyde and 1.25% glutaraldehyde pre-

pared in 0.2 M fresh phosphate buffer at 4°C. The corresponding spinal segment of the sciatic nerve was cut transversely into 30 μ m-thick serial sections using a vibratome (VT 1000S, Solms, Germany). Sections were visualized with benzidine dihydrochloride (Kennelly, 2006). Cells containing blue-stained particles in motor neurons of the anterior horn of the spinal cord were counted under a light microscope (BH-3; Olympus).

Statistical analysis

Measurement data, expressed as the mean \pm SD, were analyzed using SPSS 19.0 software (IBM Corp., Armonk, NY, USA). Groups were compared using one-way analysis of variance followed by the Student-Newman-Keuls test. $P < 0.05$ was considered statistically significant.

Results

General observation of rats after model establishment

All animals survived, and no wound infections were noted. Recovery time after anesthesia was 85 ± 2 minutes in groups A1 and A2, and 64 ± 2 minutes in groups B1 and B2. In both groups A1 and A2, appetite and activity of the rats appeared reduced. The character of stool and urine changed. One week later, the rats' food intake returned to normal, but the character of the stool and urine was not restored. Three days after surgery, redness and swelling of the feet were marked in group B2, but mild in other groups. Active flexion of the right lower limb was limited, and dorsiflexion deformity of the right foot was seen. The heel touched the ground during walking. Three weeks after model induction, varying degrees of ulceration were visible in the rat heel in groups A2, B1 and B2. No visible ulceration was detected in group A1. At 12 weeks, ulcers were mostly healed in all groups, and autophagy was noted in the feet of some rats in group B2 (Figure 1).

SFI

At 4 weeks after surgery, SFI was better in groups A1 and A2 than in groups B1 and B2 ($P < 0.01$). From the 4th week, SFI began to decrease in each group and the decreased range became more pronounced with time. At 8 and 12 weeks, SFI was better in groups A2 and B1 than in group B2 ($P < 0.01$) and better in group A1 than in all other groups ($P < 0.01$; Figure 2).

Recovery rate of action potential amplitude in sciatic nerve trunk

At 8 weeks after surgery, recovery was the best in group A1 compared with all other groups. Recovery was better in group A2 than in groups B1 and B2 ($P < 0.01$), and better in group B1 than in group B2 ($P < 0.01$). At 12 weeks after surgery, recovery was better in group A1 than in all other groups ($P < 0.01$). Groups A2 and B1 also showed better recovery than group B2 ($P < 0.01$) (Figure 3).

Recovery rate of gastrocnemius muscle wet weight

At 4 weeks after surgery, the denervated gastrocnemius muscle was paler in color than the contralateral gastrocnemius, and amyotrophy was evident in each group. At 8 and 12 weeks after surgery, recovery of the muscle was markedly

better in groups A1, A2 and B1 than in group B2 (**Figure 4**). At 4 weeks after surgery, muscle wet weight recovery rate was greater in group A1 than in all other groups ($P < 0.01$). At 8 and 12 weeks after surgery, recovery rate of gastrocnemius muscle wet weight was better in group A1 than in groups B1 and B2, and better in groups A2 and B1 than in group B2 ($P < 0.01$). At 8 weeks after surgery, recovery was better in group A2 than in group B1 ($P < 0.01$), whereas by 12 weeks after surgery, no significant difference was observed between groups A2 and B1 ($P > 0.01$) (**Figure 5**).

Masson's trichrome staining of gastrocnemius muscle

At 4 weeks after surgery, no significant difference in recovery of the muscle cross-section was observed between the different groups. At 8 and 12 weeks after surgery, however, cross-section recovery was better in group A1 than in all other groups. There was no obvious difference in recovery between groups A2 and B1, but recovery was better in groups A1, A2 and B1 than in group B2 (**Figure 6**).

Hematoxylin-eosin staining of sciatic nerves

At 4 weeks after surgery, endoneurial tube formation was induced by Schwann cell aggregation, and a few mononuclear macrophages were visible in group A1. In groups A2 and B1, aggregation of mononuclear macrophages was observed, and the endoneurial tube was not formed by distinct Schwann cells. Similarly, mononuclear macrophage aggregation was observed in group B2. At 8 weeks after surgery, regenerated axonal sprouts were uniformly distributed, and mononuclear macrophages and fibroblasts were occasionally observed in group A1. Endoneurial tube formation was induced by Schwann cell aggregation. Mononuclear macrophages and a few fibroblasts were visible in groups A2 and B1, and marked macrophage aggregation was observed in group B2. At 12 weeks after surgery, Schwann cells and regenerated axonal sprouts were uniformly distributed and a few fibroblasts were visible in group A1. Scattered fibroblasts, Schwann cells and regenerated axonal sprouts were seen in groups A2 and B1. Distinct macrophages were visible in group B2 (**Figure 7**).

Masson's trichrome staining of sciatic nerves

At 4 weeks after surgery, a large number of red-stained nerve fibers and a few green-stained fibers were observed in groups A1 and B1. Green- and red-stained fibers were uniformly distributed in group A2. No red-stained nerve fibers were noted in group B2. At 8 weeks, green- and red-stained fibers were uniformly distributed in groups A1, A2 and B1. Regenerated axons were seen in group B2. At 12 weeks after surgery, in group A1, collagen fibers were uniformly distributed and arranged along nerve fibers in a wave-like formation. Green- and red-stained fibers were uniformly distributed in groups A2 and B1. Many collagen fibers and a few regenerated axons were observed in group B2 (**Figure 8**).

Toluidine blue staining of sciatic nerves

At 4 weeks after surgery, Schwann cells formed an endoneurial tube in group A1, but not in groups A2 or B1. A large

number of mononuclear cell nuclei and scattered Schwann cell nuclei were visible in group B2. At 8 and 12 weeks after surgery, the myelin sheath in regenerated myelinated nerve fibers was thicker and more uniform in group A1 than in all other groups, and thicker in groups A2 and B1 than in group B2 (**Figure 9**), with no significant difference in thickness between groups A2 and B1.

HRP tracing of neurons in the spinal cord

Under the light microscope, dark blue HRP-positive neurons were found in the anterior horn of the spinal cord in each group (**Figure 10A**). At 8 weeks after surgery, significant differences in the number of HRP-positive particles per high-power field were observed between the groups ($P < 0.01$). The rate (stained cells/total cells $\times 100\%$) of HRP-positive neurons was higher in group A1 than in all other groups, higher in group A2 than in groups B1 and B2, and higher in group B1 than in group B2. At 12 weeks after surgery, the rate of HRP-positive neurons was significantly higher in group A1 than in all other groups ($P < 0.01$). There were more HRP-positive neurons in groups A2 and B1 than in group B2 ($P < 0.01$) (**Figure 10B**).

Discussion

Brain injury is known to promote the repair of peripheral nerve injury (Wang et al., 2014). Here, we investigated the mechanism underlying this effect by comparing it to the effects of tacrolimus, which is also known to improve nerve regeneration after injury. We found that sciatic nerve recovery was better in animals that underwent brain injury and received tacrolimus than in those that received either of those interventions alone, or no intervention, after injury. This indicates that brain injury promotes the recovery of peripheral nerve injury *via* a different mechanism of action to tacrolimus (Reddaway et al., 2012; Lu et al., 2015; Ackerman et al., 2016).

When a peripheral nerve receives a class V Sunderland lesion, the loss of innervation to the target organ results in an interruption of nutrient supply from the afferent neurons, leading to target organ atrophy, intractable ulcers in pressure areas (Wade et al., 2013; Shu et al., 2015), poorer SFI (Farjah and Fazli, 2015; Dong et al., 2016), and a decrease in target muscle wet weight (Wang et al., 2014).

Tacrolimus promotes peripheral nerve repair by a relatively well understood mechanism (Glaus et al., 2011; Mekaj et al., 2014, 2015a, b; Phillips et al., 2014; Zhao et al., 2014). It exerts its neurotrophic effects in two ways. It forms a complex with the binding region of tacrolimus binding protein (FKBP12), and then combines with the functional region of that protein, which increases the expression of growth associated protein-43 and contributes to the formation and extension of growth cones. Previous studies showed that as damaged nerves recovered after treatment with tacrolimus, action potentials began to reach target organs again, the inner diameter of the regenerated axon increased, the myelin sheath thickened, and the amplitude of action potentials increased (Mekaj et al., 2014; Carrasco et al., 2016). The present results confirmed the action of tacrolimus in the promotion of peripheral nerve recovery after injury. Rats treated with tacroli-

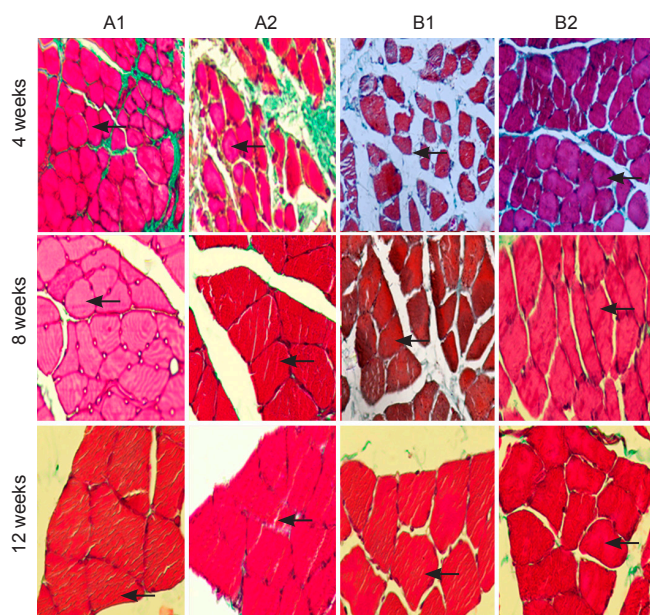


Figure 6 Masson's trichrome staining of denervated skeletal muscle with sciatic nerve injury following brain injury induction and/or tacrolimus treatment ($\times 400$).

At 4 weeks after surgery, muscular dystrophy (arrows) was observed after denervation in each group, with no notable differences between the groups. At 8 and 12 weeks after surgery, cross-section of the muscle in group A1 showed better recovery in muscular volume (arrows) than in the remaining groups. The recovery of cross-section of the muscle was better in groups A1, A2 and B1 than in group B2. Group A1: Brain injury + sciatic nerve injury + tacrolimus; group A2: brain injury + sciatic nerve injury; group B1: sciatic nerve injury + tacrolimus; group B2: sciatic nerve injury alone.

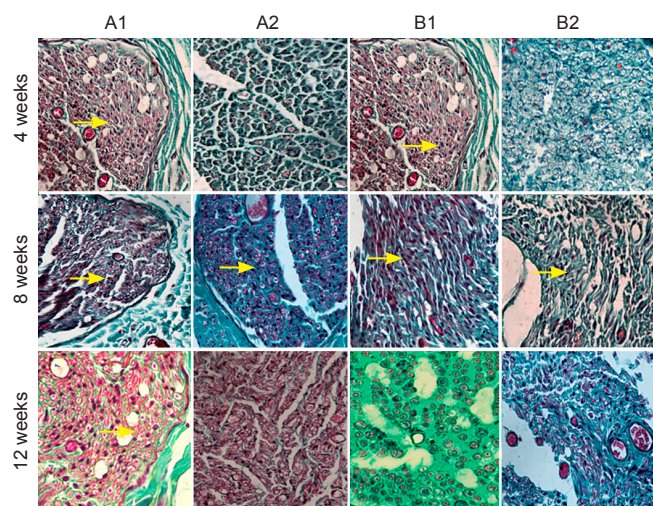


Figure 8 Masson's trichrome staining of sciatic nerves of rats with sciatic nerve injury following brain injury induction and/or tacrolimus treatment ($\times 400$).

At 4 weeks after surgery, a large number of red-stained nerve fibers and a few green-stained fibers (arrows) were observed in groups A1 and B1. At 8 weeks after surgery, green- and red-stained nerve fibers (arrows) were uniformly distributed in groups A1, A2 and B1. Regenerated axons (arrow) were seen in group B2. At 12 weeks, in group A1, collagen fibers were uniformly distributed (arrow) and arranged along nerve fibers in a wave-like formation. Group A1: Brain injury + sciatic nerve injury + tacrolimus; group A2: brain injury + sciatic nerve injury; group B1: sciatic nerve injury + tacrolimus; group B2: sciatic nerve injury alone. There were five rats in each group.

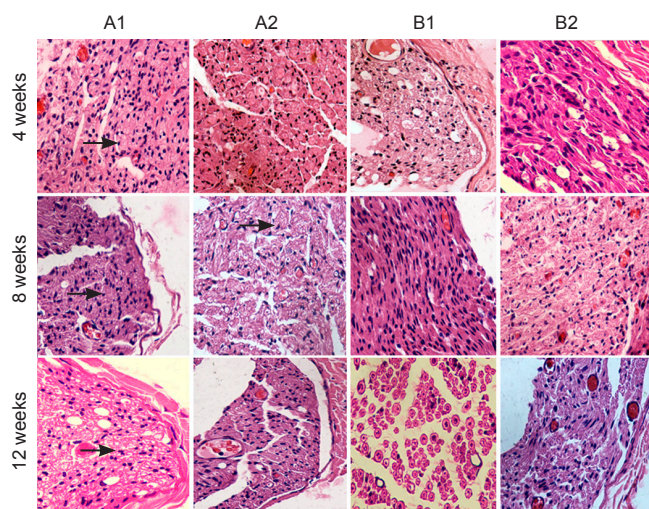


Figure 7 Hematoxylin-eosin staining of sciatic nerves of rats with sciatic nerve injury following brain injury induction and/or tacrolimus treatment ($\times 400$).

At 4 weeks after surgery, endoneurial tube formation was induced by Schwann cell aggregation (arrow), and a few mononuclear macrophages were visible in group A1. At 8 weeks, regenerated axonal sprouts were uniformly distributed (arrows), and mononuclear macrophages and fibroblasts were occasionally observed in group A1. At 12 weeks, Schwann cells and regenerated axonal sprouts were uniformly distributed (arrows) and a few fibroblasts were visible in group A1. Scattered fibroblasts, Schwann cells and regenerated axonal sprouts were seen in groups A2 and B1. Group A1: Brain injury + sciatic nerve injury + tacrolimus; group A2: brain injury + sciatic nerve injury; group B1: sciatic nerve injury + tacrolimus; group B2: sciatic nerve injury alone.

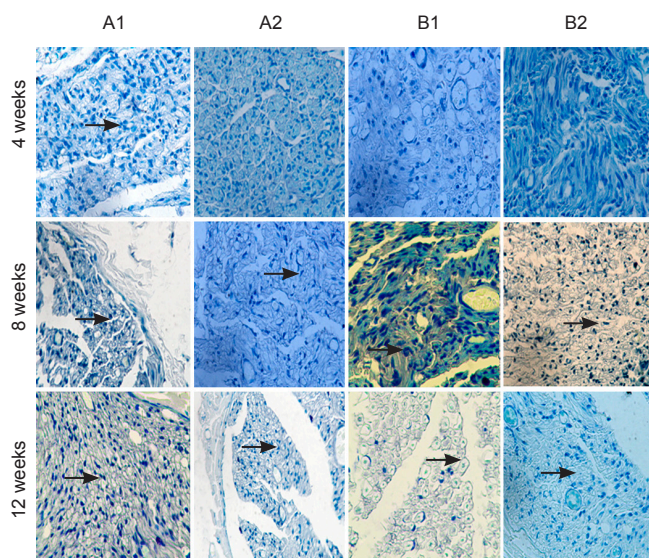


Figure 9 Toluidine blue staining of sciatic nerves of rats with sciatic nerve injury following brain injury induction and/or tacrolimus treatment ($\times 400$).

At 4 weeks after surgery, Schwann cells formed an endoneurial tube (arrow) in group A1, but not in groups A2, B1 or B2. At 8 and 12 weeks after surgery, the myelin sheath in regenerated fibers (arrows) was thicker and more uniform in group A1 than in all other groups. Group A1: Brain injury + sciatic nerve injury + tacrolimus; group A2: brain injury + sciatic nerve injury; group B1: sciatic nerve injury + tacrolimus; group B2: sciatic nerve injury alone. There were five groups in each group.

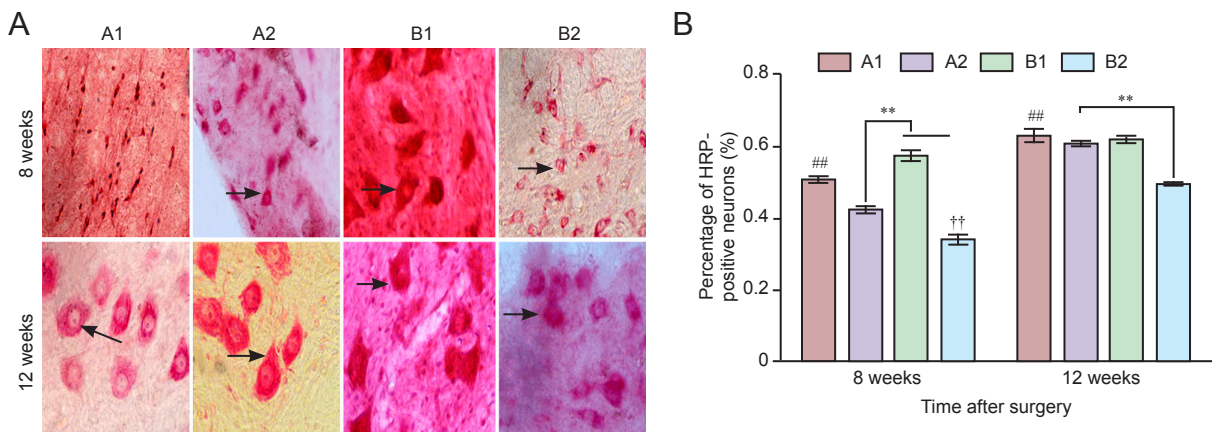


Figure 10 Horseradish peroxidase (HRP) tracing and benzidine staining of the spinal cord in rats with sciatic nerve injury following brain injury induction and/or tacrolimus treatment.

(A) Representative images of HRP tracing and benzidine staining ($\times 400$). Neuronal cells (arrows) were stained with neutral red to reveal HRP-positive particles in the cytoplasm. (B) Percentage of HRP-positive neurons (%) in the spinal cord of rats. At 8 weeks after surgery, the rate of HRP-positive neurons was higher in group A1 than in any other group ($##P < 0.01$, vs. other three groups), higher in group A2 than in groups B1 and B2 ($**P < 0.01$), and higher in group B1 than in group B2 ($\dagger\dagger P < 0.01$, vs. group B1). At 12 weeks after surgery, the rate of HRP-positive neurons was higher in group A1 than in all other groups ($##P < 0.01$, vs. other three groups), higher in group A2 than group B2 ($**P < 0.01$), and higher in group B1 than group B2 ($\dagger\dagger P < 0.01$, vs. group B1). Percentage of HRP-positive neurons = stained cells/total cells $\times 100\%$. Data expressed as the mean \pm SD were analyzed by one-way analysis of variance followed by the Student-Newman-Keuls test. Group A1: Brain injury + sciatic nerve injury + tacrolimus; group A2: brain injury + sciatic nerve injury; group B1: sciatic nerve injury + tacrolimus; group B2: sciatic nerve injury alone.

mus showed milder ulceration and improvements in SFI, gastrocnemius muscle recovery, and action potential amplitude. The effects were better in the group that received tacrolimus and brain injury than in the group that received tacrolimus without brain injury, suggesting that the mechanism by which brain injury promotes peripheral nerve repair is different from that of the tacrolimus-FKBP12 complex, which involves an increase in growth associated protein-43 expression. Further studies are needed to determine the specific mechanism.

Wallerian degeneration appeared immediately after peripheral nerve injury. Axonal fragments were engulfed by macrophages, and surviving neurons formed new axonal sprouts and extended distally. Contact with the target organ is gradually established through the endoneurial tube, which is formed by Schwann cells (Carrasco et al., 2016), and the target organ is reinnervated and nourished. Here, Masson's trichrome staining of target muscles (Mekaj et al., 2014) and sciatic nerves, toluidine blue staining, and HRP tracing all showed stronger results in group A1 than in all other groups. The likely reason for this is the immunosuppressive action of tacrolimus. The drug forms a complex by binding to FKBP12 in the cytoplasm, inhibiting CaN activity, reducing dephosphorylation of nuclear factor of activated T-cells (NFAT), and downregulating the expression of interleukins 2 and 3 and recombinant interferon, thus promoting neuronal regeneration (Glaus et al., 2011; Mekaj et al., 2015b).

Peripheral nerve injury damages the blood-nerve barrier. Macrophages and fibroblasts arrive at the site of injury, participate in the inflammatory reaction, and form a collagen scar, thus inhibiting neuronal regeneration (Konofaos and Ver Halen, 2013; Ribeiro et al., 2015). Tacrolimus reduces the local inflammatory reaction and blocks the transformation of fibroblasts, suppressing their proliferation, migration and collagen deposition, thus promoting the repair and re-

generation of damaged neurons (Gao et al., 2013). Masson's trichrome staining of nerves demonstrated that the collagen scar was smaller in group A1 than in all other groups. Regenerated axonal sprouts were connected to the endoneurial tube through the anastomotic stoma.

Schwann cells produce the myelin sheath after regulation by endogenous signals and transcription factors (Xu et al., 2016). Schwann cells also remove fragments of degenerated myelin sheath, secrete nutritional factors, create a microenvironment conducive to axonal regeneration, and promote axonal regeneration. The toluidine blue staining results showed that the myelin sheath was thicker and more regular in the brain injury + tacrolimus group than in the other groups. Neuronal cell bodies achieve the material exchange of target organs through axoplasmic transport (Lundborg et al., 1973). Regenerated axonal sprouts connect to target organs through the anastomotic stoma. The better the axonal regeneration effect, the better the functional recovery of axoplasmic transport and target organ recovery (Wang et al., 2014). In the present study, HRP tracing and Masson's trichrome staining of muscles revealed better recovery in group A1 than in all other groups.

The nervous, immune and endocrine systems are closely related (Sheth et al., 2016). When the central structure of the autonomic nervous system is damaged after brain injury, it induces alterations in the immune response and mitochondrial function in brain cells, and activates the caspase cascade, leading to neuronal apoptosis, an increase in neutrophils surrounding the site of injury, and an increase in vascular endothelial cell permeability. Therefore, immune defense and repair are stimulated through body fluids. The activated astrocytes, oligodendrocytes and neurons produce interleukin-6, causing various physiological effects and pathologic responses (Glaus et al., 2011; Mekaj et al., 2014, 2015a, b; Phillips et al., 2014; Zhao et al., 2014). These cells secrete a variety of an-

ti-inflammatory factors and neurotrophic factors to promote nerve repair (Glaus et al., 2011; Mekaj et al., 2014, 2015a, b; Phillips et al., 2014; Zhao et al., 2014). However, the mechanism for the promoting effect of brain injury on the repair of nerve injury warrants further study.

The regeneration of injured peripheral nerves remains a topic of great interest in neuroscience research. We have shown that brain injury and tacrolimus both contribute to the repair of peripheral nerve injury, but show better effects when combined. Their mechanisms of action are not identical. The precise mechanism by which brain injury promotes the repair of peripheral nerves after injury requires further exploration.

Author contributions: PW and XZH participated in study concept and design. HQW, JJM, TMH, BS, YFG, SBL, and WW provided technical and material support. XZH and PW collected and analyzed data, ensured the integrity of the data, and wrote the paper. PW and YFG served as principle investigators, were in charge of paper authorization, and obtained the funding. All authors approved the final version of the paper.

Conflicts of interest: None declared.

Research ethics: The study protocol was approved by the Ethics Committee of the Affiliated Hospital of Chengde Medical College, China (Approval number: C20160201). The experimental procedure followed the National Institutes of Health Guide for the Care and Use of Laboratory Animals (NIH Publications No. 8023, revised 1978). All efforts were made to minimize the number and suffering of the animals used in the experiments. The article was prepared in accordance with the "Animal Research: Reporting of In Vivo Experiments Guidelines" (ARRIVE Guidelines).

Open access statement: This is an open access article distributed under the terms of the Creative Commons Attribution-NonCommercial-ShareAlike 3.0 License, which allows others to remix, tweak, and build upon the work non-commercially, as long as the author is credited and the new creations are licensed under the identical terms.

Contributor agreement: A statement of "Publishing Agreement" has been signed by an authorized author on behalf of all authors prior to publication.

Plagiarism check: This paper has been checked twice with duplication-checking software iThenticate.

Peer review: A double-blind and stringent peer review process has been performed to ensure the integrity, quality and significance of this paper.

References

- Ackerman S, Smith LM, Gomes PJ (2016) Ocular itch associated with allergic conjunctivitis: latest evidence and clinical management. *Ther Adv Chronic Dis* 7:52-67.
- Carrasco DI, Seburn KL, Pinter MJ (2016) Altered terminal Schwann cell morphology precedes denervation in SOD1 mice. *Exp Neurol* 275 Pt 1:172-181.
- Cheng XL, Wang P, Sun B, Liu SB, Gao YF, He XZ, Yu CY (2015) The longitudinal epineural incision and complete nerve transection method for modeling sciatic nerve injury. *Neural Regen Res* 10:1663-1668.
- Dong HY, Jiang XM, Niu CB, Du L, Feng JY, Jia FY (2016) Cerebrolysin improves sciatic nerve dysfunction in a mouse model of diabetic peripheral neuropathy. *Neural Regen Res* 11:156-162.
- Farjah GH, Fazli F (2015) The effect of chick embryo amniotic fluid on sciatic nerve regeneration of rats. *Iran J Vet Res* 16:167-171.
- Feeney DM, Boyeson MG, Linn RT, Murray HM, Dail WG (1981) Responses to cortical injury: I. Methodology and local effects of contusions in the rat. *Brain Res* 211:67-77.
- Gao Z, Zhu Q, Zhang Y, Zhao Y, Cai L, Shields CB, Cai J (2013) Reciprocal modulation between microglia and astrocyte in reactive gliosis following the CNS injury. *Mol Neurobiol* 48:690-701.
- Glaus SW, Johnson PJ, Mackinnon SE (2011) Clinical strategies to enhance nerve regeneration in composite tissue allotransplantation. *Hand Clin* 27:495-509.
- Gold BG, Storm-Dickerson T, Austin DR (1994) The immunosuppressant FK506 increases functional recovery and nerve regeneration following peripheral nerve injury. *Restor Neurol Neurosci* 6:287-296.
- He XZ, Wang W, Hu TiM, Ma JJ, Yu CY, Gao YF, Cheng XL, Wang P (2016) Peripheral nerve repair: theory and technology application. *Zhongguo Zhuzhi Gongcheng Yanjiu* 20:1044-1050.
- Kennelly KD (2006) Electrophysiological evaluation of cranial neuropathies. *Neurologist* 12:188-203.
- Konofaos P, Ver Halen JP (2013) Nerve repair by means of tubulization: past, present, future. *J Reconstr Microsurg* 29:149-164.
- Lu YX, Su QH, Wu KH, Ren YP, Li L, Zhou TY, Lu W (2015) A population pharmacokinetic study of tacrolimus in healthy Chinese volunteers and liver transplant patients. *Acta Pharmacol Sin* 36:281-288.
- Lundborg G, Nordborg C, Rydevik B, Olsson Y (1973) The effect of ischemia on the permeability of the perineurium to protein tracers in rabbit tibial nerve. *Acta Neurol Scand* 49:287-294.
- Mekaj AY, Morina AA, Bytyqi CI, Mekaj YH, Duci SB (2014) Application of topical pharmacological agents at the site of peripheral nerve injury and methods used for evaluating the success of the regenerative process. *J Orthop Surg Res* 9:94.
- Mekaj AY, Morina AA, Lajqi S, Manxhuka-Kerliu S, Kelmendi FM, Duci SB (2015a) Biomechanical properties of the sciatic nerve following repair: effects of topical application of hyaluronic acid or tacrolimus. *Int J Clin Exp Med* 8:20218-20226.
- Mekaj AY, Morina AA, Manxhuka-Kerliu S, Neziri B, Duci SB, Kukaj V, Miftari I (2015b) Electrophysiological and functional evaluation of peroneal nerve regeneration in rabbit following topical hyaluronic acid or tacrolimus application after nerve repair. *Niger Postgrad Med J* 22:179-184.
- Phillips BZ, Franco MJ, Yee A, Tung TH, Mackinnon SE, Fox IK (2014) Direct radial to ulnar nerve transfer to restore intrinsic muscle function in combined proximal median and ulnar nerve injury: case report and surgical technique. *J Hand Surg Am* 39:1358-1362.
- Reddaway RB, Davidow AW, Deal SL, Hill DL (2012) Impact of chorda tympani nerve injury on cell survival, axon maintenance, and morphology of the chorda tympani nerve terminal field in the nucleus of the solitary tract. *J Comp Neurol* 520:2395-2413.
- Ribeiro J, Pereira T, Caseiro AR, Armada-da-Silva P, Pires I, Prada J, Amorim I, Amado S, Franca M, Goncalves C, Lopes MA, Santos JD, Silva DM, Geuna S, Luis AL, Mauricio AC (2015) Evaluation of biodegradable electric conductive tube-guides and mesenchymal stem cells. *World J Stem Cells* 7:956-975.
- Schiaveto de Souza A, da Silva CA, Del Bel EA (2004) Methodological evaluation to analyze functional recovery after sciatic nerve injury. *J Neurotrauma* 21:627-635.
- Sheth RU, Cabral V, Chen SP, Wang HH (2016) Manipulating bacterial communities by in situ microbiome engineering. *Trends Genet* 32:189-200.
- Shu B, Xie JL, Xu YB, Lai W, Huang Y, Mao RX, Liu XS, Qi SH (2015) Effects of skin-derived precursors on wound healing of denervated skin in a nude mouse model. *Int J Clin Exp Pathol* 8:2660-2669.
- Wade CE, Baer LA, Wu X, Silliman DT, Walters TJ, Wolf SE (2013) Severe burn and disuse in the rat independently adversely impact body composition and adipokines. *Critical Care* 17:R225.
- Wang W, Gao J, Na L, Jiang H, Xue J, Yang Z, Wang P (2014) Craniocerebral injury promotes the repair of peripheral nerve injury. *Neural Regen Res* 9:1703-1708.
- Xu Z, Yang B, Zhang J, Zheng J (2016) The regulation of sGC on the rat model of neuropathic pain is mediated by 5-HT_{1A}Rs and NO/cGMP pathway. *Am J Transl Res* 8:1027-1036.
- Zhao J, Zheng X, Fu C, Qu W, Wei G, Zhang W (2014) FK506-loaded chitosan conduit promotes the regeneration of injured sciatic nerves in the rat through the upregulation of brain-derived neurotrophic factor and TrkB. *J Neurol Sci* 344:20-26.

Copypedited by Li CH, Song LP, Zhao M